

Comparative Study of Composite Membranes from Nano-Metal-Oxide-Incorporated Polymer Electrolytes for Direct Methanol Alkaline Membrane Fuel Cells

Rajangam Vinodh, Dharmalingam Sangeetha

Department of Chemistry, Anna University, Chennai 600025, Tamil Nadu, India

Correspondence to: D. Sangeetha (E-mail: sangeetha@annauniv.edu)

ABSTRACT: A series of six composite membranes was prepared with two polymer electrolytes and three inorganic fillers, namely, silica, titania, and zirconia by a solution casting method. Two polymer electrolytes, that is, anion-exchange membranes, were prepared from polystyrene-*block*-poly(ethylene-*ran*-butylene)-*block*-polystyrene (PSEBS) and polysulfone by chloromethylation and quaternization. A preliminary characterization of the ionic conductivity, methanol permeability, and selectivity ratio was done for all of the prepared composite membranes to check their suitability to work in direct methanol alkaline membrane fuel cells (DMAMFCs). The DMAMFC performance was analyzed with an in-house fabricated single cell unit with a 25-cm² area. Maximum performance was achieved for the composite membrane quaternized PSEBS/7.5% TiO₂ and was 74.5 mW/cm² at 60°C. For the comparison purposes, a commercially available anion-exchange membrane (Anion Membrane International-7001) was also investigated throughout the study. © 2012 Wiley Periodicals, Inc. *J. Appl. Polym. Sci.* 000: 000–000, 2012

KEYWORDS: batteries and fuel cells; composites; electrochemistry

Received 17 March 2012; accepted 26 June 2012; published online

DOI: 10.1002/app.38266

INTRODUCTION

The direct methanol alkaline membrane fuel cell (DMAMFC) is another fuel cell that has generated interest with regard to portable electronic devices with the potential to offer 10 times higher power densities than current lithium-ion rechargeable batteries. Although there are several different types of fuel cells, the DMAMFC offers the most promising alternative for portable power applications because it is a low-temperature device, it is environmentally benign, and its fuel is portable and inexpensive. Therefore, considerable research effort has been focused on miniaturizing and improving the efficiency of the DMAMFC. Nafion membrane appears to be a popular membrane electrolyte for direct methanol fuel cell (DMFC) or proton electrolyte membrane fuel cell (PEMFC) applications. However, at present, two major technical problems in DMFCs still restrict their performance and application. One problem is the crossover of methanol through the electrolyte membrane. The other is the slow methanol oxidation kinetics on the anode catalyst. Moreover, the high cost of Nafion membranes impede the market penetration of DMFCs. Research and developmental activities have focused keen interest on the development of alternative polymer electrolyte membranes,¹ but little interest has been shown in alkaline-based membranes.^{2,3}

It has been known for a long time that the anodic oxidation of methanol in alkaline media is more feasible than in acidic media.^{4–6} Then, whereas most researchers have tried every possible way to improve the performance of DMFCs, an increasing number of researchers are turning their interest to DMAMFCs.^{5–11} Compared to DMFCs in acidic media, DMAMFCs have a number of potential advantages.^{7–12} First, it is well known that methanol oxidation in alkaline media is kinetically faster than that in acidic media. Second, methanol oxidation catalysts are less sensitive in alkaline media than in acidic media; this could lead to the use of less expensive non-precious metal catalysts, such as Ni or Ag. In addition, the charge carrier in DMAMFCs is an anion, and it moves from the cathode to the anode during fuel cell operation; this is opposite to the movement of protons in acidic membranes. As such, the direction of the electro-osmotic drag is reversed, and this reduces the methanol permeation rate.

To date, various anion-exchange membranes (AEMs) have been synthesized and characterized, including grafted polymers,^{9,13} crosslinked copolymers,^{14,15} random copolymers,^{16–18} pyridinium-type polymers,¹⁹ and block copolymers.^{20,21} Note that despite different AEM chemical structures, the covalently attached cations in all of these polymers were based on ammonium. So

far, among all of the cations investigated, the quaternary ammonium cation has received the most attention. Other cations in AEMs have also been recently investigated, including phosphonium,²² sulfonium,²³ guanidinium,²⁴ and imidazolium.^{25–27}

In the past, very limited literature reports were made to develop anionic composite membranes with metal oxides as fillers for alkaline fuel cells. Wang et al.²⁸ prepared a hybrid polymer membrane for an alkaline direct ethanol fuel cell based on poly(vinyl alcohol) and 3-(trimethyl ammonium) propyl functionalized silica (designated as Q–SiO₂). The highest reported peak power density of direct ethanol fuel cells with an alkaline composite hybrid membrane was 50 mW/cm² at 60°C. Wu et al.²⁹ synthesized silica/poly(2,6-dimethyl-1,4-phenylene oxide) hybrid AEM for alkaline fuel cells and obtained a peak power density of 32 mW/cm² at 50°C.

So far, to the best of our knowledge, no attempt has been made to develop composite polymer electrolyte membranes based on quaternized polystyrene-*block*-poly(ethylene-*ran*-butylene)-*block*-polystyrene (QPSEBS)²⁰ and quaternized polysulfone (QPSU)^{30,31} with inorganic additives for DMAMFC applications. In the following account, the fabrication, ionic conductivity, methanol permeability, selectivity ratio, and DMAMFC performances of the prepared QPSEBS and QPSU composite membranes are discussed. In this study, we focused on low cost, good mechanical stability, adequate ionic conductivity, and lower methanol permeability to satisfy the needs of DMAMFCs.

EXPERIMENTAL

Materials

Silica (10–15 nm; CAS no. 7631-86-9), titania (10–15 nm; CAS no. 13463-67-7), and zirconia (10–15 nm; CAS no. 1314-23-4), with a purity of 99% each, were purchased from Sigma Aldrich (USA). Other chemicals, including cyclohexane, methanol, sodium hydroxide, potassium hydroxide, and dimethylformamide, were purchased from E-Merck (India). All were analytical grade and were used as received. Pt and Pt–Ru on a carbon support were purchased from Arora-Mathey Pvt., Ltd. (India). Polytetrafluoroethylene binder (CAS No. 9002-84-0, 60 wt % dispersion in water) and isopropyl alcohol were purchased from Sigma-Aldrich. Carbon cloth was obtained from Cobat Carbon, Inc. (Germany). The Anion Membrane International-7001 (AMI-7001) AEM was purchased from Membranes International, Inc. The important properties of AMI-7001 are given in Table I. All of the experiments were carried out with double-distilled water.

Fabrication of the Composite Membrane

The polymer electrolytes, that is, QPSEBS and QPSU, were dissolved in their respective solvents, cyclohexane and dimethylformamide. Different proportions (2.5, 5, 7.5, and 10%) of inorganic nanofillers (TiO₂, SiO₂, and ZrO₂) were added to this solution and stirred for about 24 h. Each solution was then subjected to ultrasonication for about 15 min, subsequently poured onto a clean Petri dish, and dried at 60°C for 8 h to obtain the membrane with desired thickness.³¹

Ionic Conductivity

The ionic conductivity of the membrane was determined with alternating-current impedance spectroscopy. Before testing, the

Table I. Important Properties of the AMI-7001 Membrane

Functionality	Strong base AEM
Polymer structure	Polystyrene crosslinked with divinylbenzene
Functional group	Quaternary ammonium group
Thickness	450 ± 25 μm
Ion-exchange capacity	1.3 ± 1 mequiv/g
Water absorption	17%
Ionic conductivity	1.72 × 10 ⁻² S/cm
Thermal stability	90°C
Chemical stability range	pH = 1–10

OH⁻ form of the membrane was hydrated in deionized water for 24 h. The testing device with the membrane was placed in deionized water to maintain the relative humidity at 100% during the measurements. From the difference between the resistance of the blank cell and the one with membrane separating the working and counter-electrode compartments, the resistance of the membrane was calculated and converted to conductivity values with the following formula:

$$\text{Conductivity} = L/RA$$

where R is the sample resistance (Ω), L is the wet sample thickness (cm), and A is the sample area (cm²).

Methanol Permeability

Methanol permeability measurements^{32,33} were carried out with a diffusion cell. The diffusion cell was divided into two chambers, in which one chamber (compartment B) was filled with deionized water and the other chamber (compartment A) was filled with 20 wt % methanol mixed with a 1M KOH aqueous solution. Before testing, the prepared membranes were hydrated in deionized water for at least 24 h. A membrane with a particular surface area (square centimeters) was sandwiched by O-rings and clamped tightly between two bottles or compartments. A magnetic pellet was kept active in the glass diffusion cell during the experiment. The concentration of methanol diffused from compartment A to compartment B across the membrane was examined with a digital refractometer (Atago India Instruments Pvt. Ltd., Mumbai, India). An aliquot of 0.20 mL was sampled from compartment B every 15 min. Before the permeation experiment, a calibration curve for the value of density versus the methanol concentration was prepared. The calibration curve was used to determine the methanol concentration in the permeation experiment. The methanol permeability was calculated from the slope of the straight-line plot of methanol concentration versus permeation time. The methanol concentration in compartment B as a function of time is given in the following equation:

$$C_B(t) = (A/V)(DK/L)C_A(t - t_0)$$

where C is the methanol concentration (mol/L), A and L are the polymer membrane area (cm²) and thickness (mm), respectively, and D and K are the methanol diffusivity and partition coefficient between the membrane and the solution, respectively.

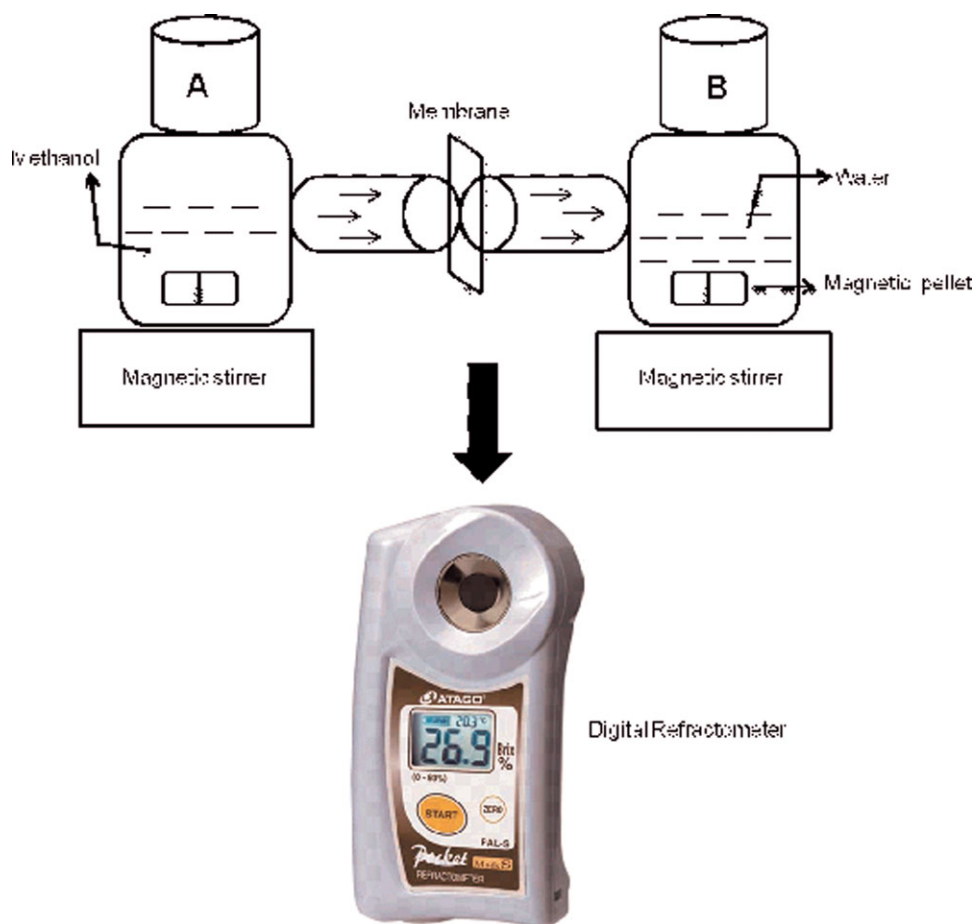


Figure 1. Schematic representation of the methanol permeability setup. [Color figure can be viewed in the online issue, which is available at wileyonlinelibrary.com.]

V and t are the volume of methanol solution (mL) and time (s) respectively. The product DK is the membrane permeability (P), and t_0 , the time lag, is related to the diffusivity (D) as follows:

$$t_0 = L^2/6D$$

A schematic representation of the methanol permeability setup is shown in Figure 1.

Selectivity Ratio

An electrolyte membrane, particularly for DMAMFC, should have two important properties: the ionic conductivity should be maximum, and the methanol diffusion should be minimum. Hence, the higher the ratio of the ionic conductivity to the methanol permeability (referred to as the *selectivity ratio*) is, the better the membrane performance in DMAMFCs will be. This selectivity ratio is an indication about the performance of the electrolyte membrane.

Hydrolytic and Alkaline Stability Tests

The boiling water test (hydrolytic stability test) was carried out by immersion of the membrane in water and the heating of the water to its boiling point, whereas in the alkaline stability test, the membrane was immersed in a 5M sodium hydroxide solution over a period of time.

An alkaline stability test (or durability test) was performed to analyze the durability of the membrane in the fuel cell condition. The durability of the polymer membrane, which undergoes degradation normally when a fuel cell is operated, can be determined with this method. This test helps to accelerate the degradation process; this thereby indicates the mechanical and chemical stability of the membrane over a long period of time in the fuel cell operating conditions.

Fabrication of the Membrane Electrode Assembly (MEA) for CH₃OH/O₂ Fuel Cells

The MEA is one of the most important components impacting the overall performance of DMAMFCs. The MEA structure is composed of an electrolyte membrane coated by a catalyst on both the anode and cathode sides and sandwiched by a gas diffusion layer. Carbon cloth is the most widely used material for the gas diffusion layer. After the preparation of the diffusion layer, catalyst slurry ink was prepared with the help of carbon-supported Pt–Ru (Pt–Ru/C) and Pt (Pt/C) catalyst with loadings of 0.5 and 0.375 mg/cm², respectively, for the anode and cathode, respectively. Then, a suitable amount of double-distilled water and isopropyl alcohol were mixed well with an ultrasonicator (Model Equitron, India). After ultrasonication, the black catalyst slurry was coated onto the respective diffusion

Table II. Experimental Conditions for MEA and DMAMFC Operation

DMAMFC	Anode	Cathode
Catalyst	Pt-Ru/C	Pt/C
Catalyst loading (mg/cm ²)	0.375	0.5
Active area (cm ²)	25	25
Fuel/oxidant	2M CH ₃ OH + 1M KOH	O ₂
Flow rate (mL/min)	20	40
Relative humidity (%)	77	77
Cell temperature (°C)	60	60

layers. The prepared anode and cathode were dried in a vacuum oven at 100°C for 2 h and then in a muffle furnace at 350°C for 6 h (Table II). The prepared composite membranes were sandwiched between the prepared anode and cathode electrodes and hot-pressed at 80°C at a 1.5-ton pressure for 2 min.

Fuel Cell Performance Study

The basic cell consisted of an AEM sandwiched between the two electrodes. The fuel cell was supplied with 2M methanol with 1M KOH as a fuel into the anode and oxygen as an oxidant into the cathode with a constant flow rate of 20 and 40 mL/min, respectively, at 60°C under ambient pressure condi-

tions. Methanol at the anode released six protons along with six electrons and CO₂. The released electrons passed through an external circuit to reach the cathode. Simultaneously, the OH⁻ diffused through the membrane to the cathode to react with oxygen and the returning electron. CO₂ and water were the products produced at the anode.

The direct-current voltage current source was used to monitor the electrical current from the cell. The experiment was conducted with 2M methanol at a flow rate of 20 mL/min in the anode side, and in the cathode side, O₂ with a flow rate of 40 mL/min was maintained. The produced current was monitored with a direct-current voltmeter (K-PAS, India). A polarization curve was drawn with current density on the *x* axis and the obtained voltage on the *y* axis. The pictorial representations of the assembled DMAMFC setup and its electrochemical reaction are shown in Figure 2.

RESULTS AND DISCUSSION

QPSEBS and Its Metal Oxide Composites

Ionic Conductivity. *Ionic conductivity* is defined as the capability of the transportation of ions that determines the power generation of a fuel cell. With the introduction of quaternary ammonium groups to the polymer chain, the hydroxyl ion conducting ability was introduced. Impedance value measurement of the ion-exchange membranes at room temperature and

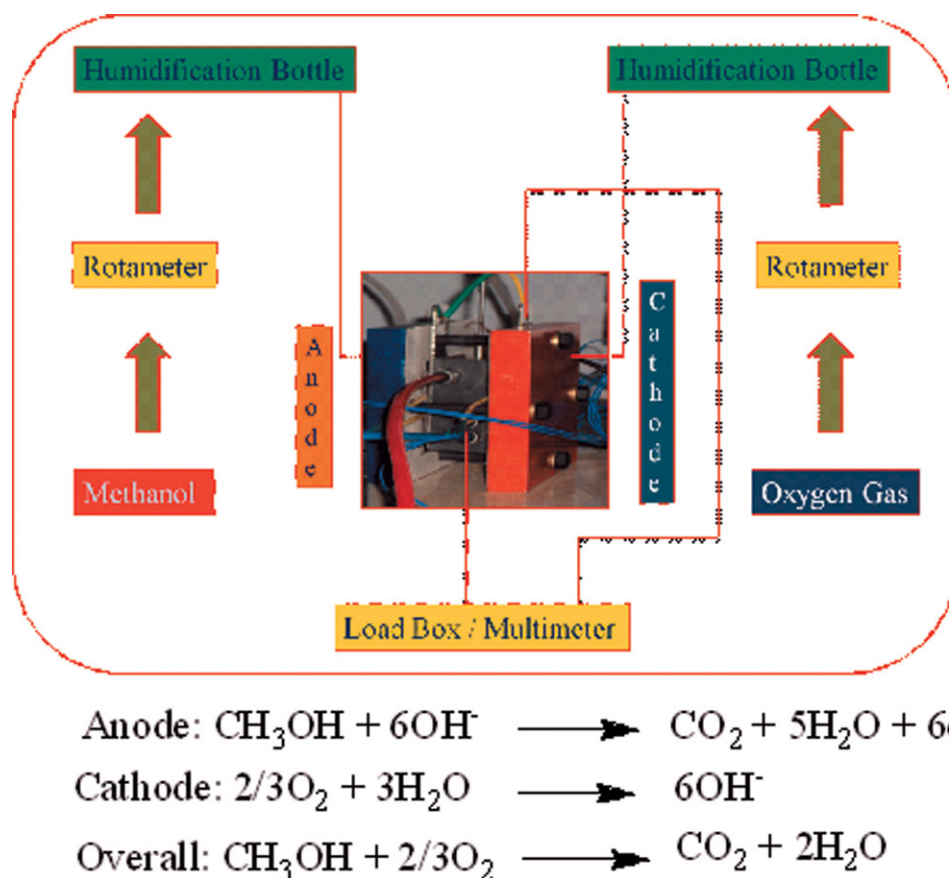


Figure 2. Pictorial representations of the assembled DMAMFC setup and its electrochemical reaction. [Color figure can be viewed in the online issue, which is available at wileyonlinelibrary.com.]

Table III. Ionic Conductivity, Methanol Permeability, and Selectivity Ratio Values of QPSEBS and Its Metal Oxide Composite Membranes

Membrane	Ionic conductivity (S/cm)	Methanol permeability (cm ² /s)	Selectivity ratio (Ss/cm ³)
AMI-7001	1.72×10^{-2}	2.25×10^{-6}	0.76×10^4
QPSEBS	1.51×10^{-2}	2.14×10^{-6}	0.71×10^4
QPSEBS/2.5% TiO ₂	1.63×10^{-2}	2.06×10^{-6}	0.79×10^4
QPSEBS/5% TiO ₂	1.69×10^{-2}	1.87×10^{-6}	0.90×10^4
QPSEBS/7.5% TiO ₂	1.78×10^{-2}	1.76×10^{-6}	1.01×10^4
QPSEBS/10% TiO ₂	1.74×10^{-2}	1.75×10^{-6}	0.99×10^4
QPSEBS/2.5% SiO ₂	1.67×10^{-2}	2.11×10^{-6}	0.79×10^4
QPSEBS/5% SiO ₂	1.73×10^{-2}	2.03×10^{-6}	0.85×10^4
QPSEBS/7.5% SiO ₂	1.81×10^{-2}	1.89×10^{-6}	0.96×10^4
QPSEBS/10% SiO ₂	1.86×10^{-2}	1.82×10^{-6}	1.02×10^4
QPSEBS/2.5% ZrO ₂	1.69×10^{-2}	2.03×10^{-6}	0.83×10^4
QPSEBS/5% ZrO ₂	1.77×10^{-2}	1.97×10^{-6}	0.90×10^4
QPSEBS/7.5% ZrO ₂	1.80×10^{-2}	1.90×10^{-6}	0.95×10^4
QPSEBS/10% ZrO ₂	1.84×10^{-2}	1.79×10^{-6}	1.03×10^4

100% humidity was taken. To examine the conductivity, the quaternized membrane and corresponding composite membranes were first soaked in a 1M KOH solution for 24 h to convert it into an OH⁻ form, and then, it was washed several times with deionized water. After the free KOH was completely removed, the conductivity of the membrane was measured. The conductivity values are shown in Table III. The ionic conductivity of the membrane increased with increasing inorganic filler content. This may have been due to the higher number of water molecules adsorbed by the nanofillers, which promoted the Grothus and vehicle-type mechanisms. A higher amount of adsorbed water molecules solvated the moieties of a polymer to a greater extent and became responsible for the higher ionic conductivity. The composite membrane with 10 wt % SiO₂ showed a higher conductivity of 1.86×10^{-2} S/cm at 100% hydrated condition, among all of the studied membranes.

Methanol Permeability and Selectivity Ratio. The methanol permeability is the product of the diffusion coefficient and sorption coefficient, in which the diffusion coefficient reflects the effect of the surrounding environment on the molecular motion of the permanent and the sorption coefficient correlates the concentration of a component in the fluid phase.^{34,35}

The ionic conductivity and methanol permeability are the two electrochemical properties that determine the efficiency of DMAMFCs. When the quaternized polymer membrane contacts the aqueous medium, OH⁻ ions can combine with water molecules and form a complex. Quaternary ammonium groups create effective pathways for the transportation of ions. However, in the meanwhile, the methanol molecule can also permeate through the broad hydrophilic channels that are created for the ion migration.^{36,37} So a considerable effort has to be devoted to achieving high ionic conductivity and lower methanol permeability for high-efficiency DMAMFC performance.

The methanol permeability of the QPSEBS membrane was found to be 2.14×10^{-6} cm²/s in a 2M methanol solution, whereas the commercially available AEM (AMI-7001) had a

methanol permeability of 2.25×10^{-6} cm²/s. However, Nafion, a cation-exchange membrane, had a methanol permeability of 2.23×10^{-7} cm²/s. This showed that the methanol permeabilities of the QPSEBS and AMI-7001 membrane were approximately one order of magnitude lower than that of the Nafion membrane. It was probably that the polystyrene-*block*-poly(ethylene-ran-butylene)-*block*-polystyrene (PSEBS) matrix had less methanol affinity than the perfluorinated hydrocarbon polymer, and the nonionic block could act as a barrier to methanol.

Low methanol permeability is an important requirement for a membrane in DMAMFCs. The results of methanol permeability of the composite membranes based on QPSEBS and its metal oxide composites are shown in Table III. It is evident from Table III that the methanol permeability decreased with the incorporation of metal oxides (TiO₂, SiO₂, and ZrO₂) in the quaternized polymer matrix. It is known that methanol permeates through hydrophilic ionic channels and that OH⁻ ions are transported by hopping between ionic sites. Therefore, the methanol permeability decreases because of the incorporation of metal oxides, which act as a material for blocking methanol transport, whereas the ionic conductivity increases.

In DMAMFC applications, the ratio of the ionic conductivity to methanol permeability (selectivity ratio) is a characteristic parameter for evaluating the fuel cell performances of membranes. In general, membranes with a higher ionic conductivity and lower methanol permeability are more suitable for DMAMFCs. The selectivity ratios of QPSEBS and AMI-7001 were found to be 0.71×10^4 and 0.76×10^4 Ss/cm³, respectively. In the case of the composites, QPSEBS/10% ZrO₂ exhibited a higher selectivity ratio (1.03×10^4 Ss/cm³) than the rest. A higher selectivity ratio is favored for DMAMFC operation. The composite membrane possessed a greater selectivity ratio than the AMI-7001 membrane and could have a great impact on the DMAMFC field.

Hydrolytic and Alkaline Stability. The hydrolytic stability of the membranes was investigated by the introduction of the

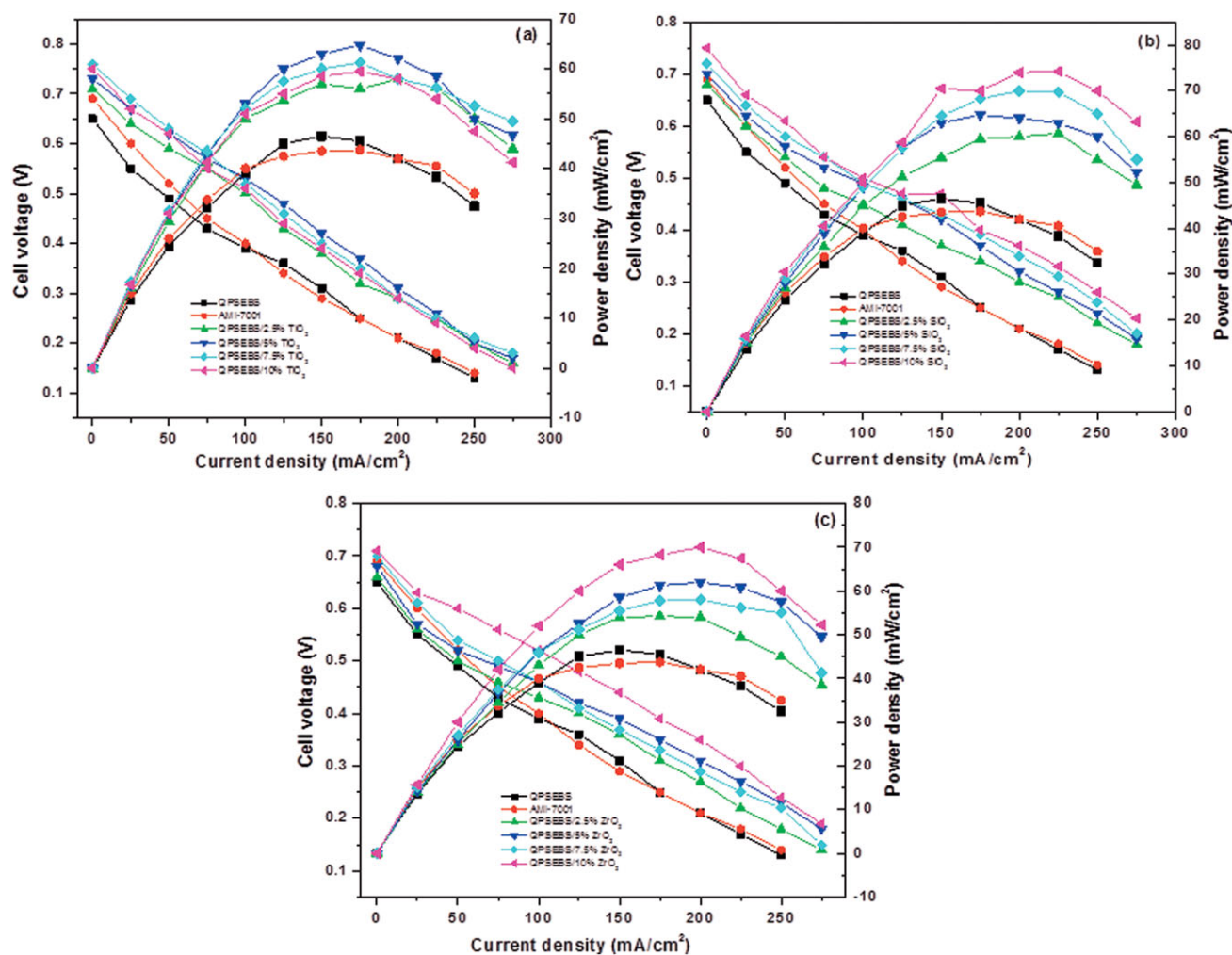


Figure 3. DMAMFC performance curves of (a) QPSEBS/TiO₂, (b) QPSEBS/SiO₂, and (c) QPSEBS/ZrO₂ with AMI-7001. [Color figure can be viewed in the online issue, which is available at wileyonlinelibrary.com.]

membranes into boiling water. It was found that the QPSEBS and nanocomposite membranes withstood the boiling water conditions without any physical deformation; this indicated that the polymer structures of QPSEBS and the nanocomposite membranes had good hydrolytic stability. Hence, these results clearly reveal that the prepared composite membranes possessed good mechanical and chemical stabilities for use in fuel cells.

DMAMFC Performance Study

The DMAMFC performance of the QPSEBS, AMI-7001, and QPSEBS/metal oxide composites was investigated with Pt–Ru/C and Pt/C as the anode and cathode catalysts, respectively, as depicted in Figure 3. The current–voltage curves showed improved performance in the QPSEBS/metal oxide composites compared to the bare QPSEBS and AMI-7001 membranes when the DMAMFC was operated at 60°C. The open-circuit voltage (OCV) of QPSEBS was found to be 0.65 V, and a maximum power density of 46.5 mW/cm² was achieved at a current density of 150 mA/cm², whereas AMI-7001 showed an OCV of 0.69 V and a maximum power density value of 43.75 mW/cm² at 60°C. However, among all of the other composite mem-

branes, maximum performance was obtained from QPSEBS/10% SiO₂, that is, the maximum OCV was found to be 0.75 V, and a maximum power density of 74.25 mW/cm² was found at a current density of 175 mA/cm². Hence, the composite membranes prepared from TiO₂, SiO₂, and ZrO₂ were preferably used in DMAMFCs.

QPSU and its Metal Oxide Composites

Ionic Conductivity. One of the most important parameters that govern the suitability of a polymer electrolyte membrane for use in fuel cells is its ionic conducting ability. The ionic conductivity of pristine QPSU (Table IV) was found to be 0.72×10^{-2} S/cm. In the case of the composites, there was an increase in the ionic conductivity with increasing content of metal oxides, that is, TiO₂, SiO₂, and ZrO₂. This increasing trend could be explained by the presence of metal oxides that acted as Lewis acid sites to provide extra water to the membrane. Also, the membrane ionic conductivity was affected by the ion concentration and mobility, hydration levels, and polymer structure or chain mobility.³⁸ To date, the influence of metal oxide components on the membrane conductivity has

Table IV. Ionic Conductivity, Methanol Permeability, and Selectivity Ratio Values of QPSU and Its Metal Oxide Composite Membranes

Membrane	Ionic conductivity (S/cm)	Methanol permeability (cm ² /s)	Selectivity ratio (Ss/cm ³)
AMI-7001	1.72×10^{-2}	2.25×10^{-6}	0.76×10^4
QPSU	0.72×10^{-2}	2.63×10^{-6}	0.27×10^4
QPSU/2.5% TiO ₂	0.80×10^{-2}	2.51×10^{-6}	0.32×10^4
QPSU/5% TiO ₂	0.93×10^{-2}	2.27×10^{-6}	0.41×10^4
QPSU/7.5% TiO ₂	1.05×10^{-2}	2.01×10^{-6}	0.52×10^4
QPSU/10% TiO ₂	1.24×10^{-2}	1.92×10^{-6}	0.65×10^4
QPSU/2.5% SiO ₂	0.98×10^{-2}	2.32×10^{-6}	0.42×10^4
QPSU/5% SiO ₂	1.17×10^{-2}	2.14×10^{-6}	0.55×10^4
QPSU/7.5% SiO ₂	1.39×10^{-2}	1.94×10^{-6}	0.72×10^4
QPSU/10% SiO ₂	1.63×10^{-2}	1.86×10^{-6}	0.88×10^4
QPSU/2.5% ZrO ₂	0.86×10^{-2}	2.39×10^{-6}	0.36×10^4
QPSU/5% ZrO ₂	0.98×10^{-2}	2.18×10^{-6}	0.45×10^4
QPSU/7.5% ZrO ₂	1.22×10^{-2}	1.92×10^{-6}	0.64×10^4
QPSU/10% ZrO ₂	1.51×10^{-2}	1.74×10^{-6}	0.87×10^4

been investigated extensively and debated, but there is still no agreement. On the one hand, a crosslinked metal–O–metal network may limit the mobility of the conductive ions and hinder

the formation of conductive and hydrophilic ionic clusters and channels (as found with the perfluorosulfonic acid polymer electrolytes) and, thus, decrease the ionic conductivity.^{39,40} On

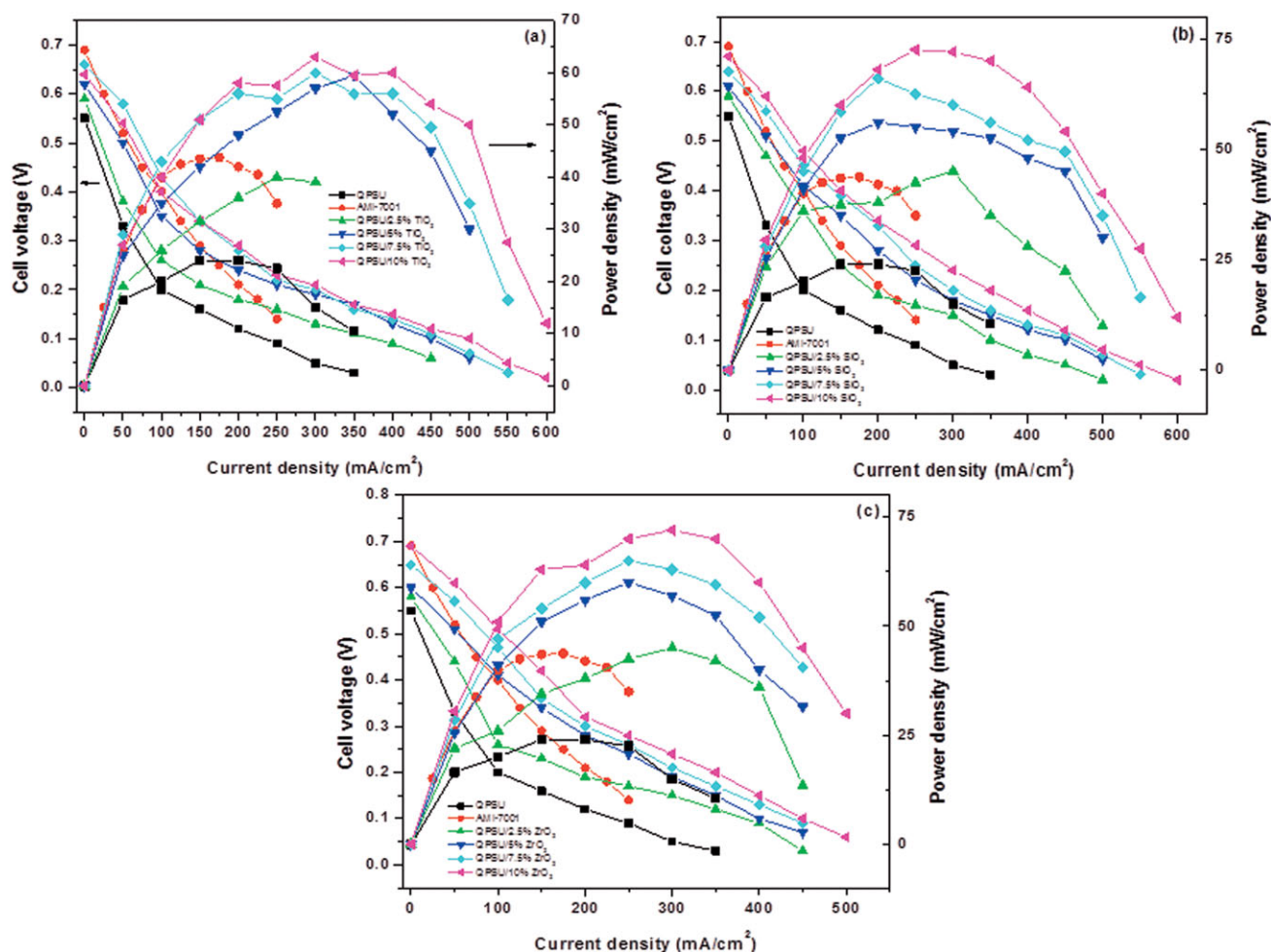


Figure 4. DMAMFC performance curves of (a) QPSU/TiO₂, (b) QPSU/SiO₂, and (c) QPSU/ZrO₂ with AMI-7001. [Color figure can be viewed in the online issue, which is available at www.interscience.wiley.com.]

the other hand, hydroxyl groups [–metal (OH)] from metal oxides have a strong bonding ability with H₂O molecules; this favors water retention and, therefore, ion transfer.⁴¹ Hence, an increase in ionic conductivity with increasing content of metal oxides in this study could be explained by the formation of metal bonds (–OHs) from metal oxides.

Methanol Permeability and Selectivity Ratios. The methanol permeability of AMI-7001 was tested for comparison purposes and was found to be 2.25×10^{-6} cm²/s (Table IV). When compared with AMI-7001, the permeation of methanol in the case of QPSU was higher. However, with the introduction of inorganic fillers, there was a remarkable decrease in the methanol permeability. The resistivity to the flow of methanol in the case of the composites became better than those of QPSU and AMI-7001 when the concentration of metal oxide went beyond 5 wt %.

The selectivity ratios of the AMI-7001, pristine QPSU, and composite membranes are given in Table IV. The pristine QPSU electrolyte membrane exhibited a selectivity ratio of 0.27×10^4 Ss/cm³; this was lower than that of AMI-7001. On the other hand, the composite membranes exhibited a comparable selectivity ratio with AMI-7001. This indicated that there was an excellent reduction in the methanol permeation at the expense of a meager amount of ionic conductivity.

Hydrolytic and Alkaline Stabilities. The property of ion exchange capacity (IEC) was measured after the hydrolytic and alkaline stability tests. The entire membranes exhibited a loss of IEC ranging from 0.76 to 1.73% only. Hence, these membranes possessed good mechanical and chemical stabilities and were also viable candidates for working in fuel cell applications.

DMAMFC Performance Study

The polarization and power density curves of QPSU and the composite membranes, obtained from the DMAMFC with Pt–Ru/C as the anode and Pt/C as cathode catalyst, are presented in Figure 4. We made the measurements by feeding methanol and oxygen as a fuel and oxidant, respectively, at 60°C. The DMAMFC with the QPSU/10% SiO₂ composite membrane gave better performance than those with QPSU, AMI-7001, and other composite materials in terms of both OCV and power density. The OCV of QPSU/10% SiO₂ was 0.69 V. The power density of the cell increased with the current density and presented a maximum power density of 72.5 mW/cm² for 10% SiO₂. The increased fuel cell performance was due to the incorporation of hygroscopic metal oxide fillers. Metal oxide species improved the mechanical properties of the membranes because specific interactions between inorganic and organic components improve water management.⁴² Moreover, the inorganic particles form a new membrane structure inhibits the direct permeation of reaction gases.⁴³ Furthermore, higher peak power densities are anticipated with the use of thinner membrane samples (<70 μm) and optimized electrodes (coated in ionomers that had better chemical compatibility to the membranes). A lower membrane thickness was achieved with the adjustment of the concentration and viscosity of the casting solution and the choice of suitable Petri dishes.

CONCLUSIONS

Collectively, it could be inferred that the various inorganic fillers used to fabricate composite membranes showed good ionic conductivity; this is very important for consideration as an electrolyte in fuel cells.

From this investigation, we concluded that the composite membranes acted as an excellent replacement for the commercially available AEM (AMI-7001) in DMAMFC because of the appreciable reduction in the methanol permeation and the higher selectivity ratio of this membrane compared to QPSEBS and QPSU.

They offered a better output in the DMAMFC compared to AMI-7001, virgin QPSEBS, and QPSU.

Maximum performance was achieved for the QPSEBS/7.5% TiO₂ composite membrane, 74.5 mW/cm² at 60°C.

ACKNOWLEDGMENTS

Financial support from the Department of Science and Technology, New Delhi, India (letter number SR/S2/CMP-06/2008, dated August 21, 2008), is gratefully acknowledged.

REFERENCES

- Liu, Y. J.; Jian, X. G.; Liu, S. J. *J. Appl. Polym. Sci.* **2001**, *82*, 823.
- Zhang, H.; Zhou, Z. *J. Appl. Polym. Sci.* **2008**, *110*, 1756.
- Varcoe, J. R.; Slade, R. C. T. *Fuel Cells* **2005**, *5*, 187.
- Parsons, R.; VanderNoot, T. J. *Electroanal. Chem.* **1988**, *257*, 9.
- Tripković, A. V.; Popović, K. D.; Grgur, B. N.; Blizanac, B.; Ross, P. N.; Marković, N. M. *Electrochim. Acta.* **2002**, *47*, 3707.
- Prabhuram, J.; Manoharan, R. *J. Power Sources* **1998**, *74*, 54.
- Yu, E. H.; Scott, K. *J. Power Sources* **2004**, *137*, 248.
- Danks, T. N.; Slade, R. C. T.; Varcoe, J. R. *J. Mater. Chem.* **2002**, *12*, 3371.
- Danks, T. N.; Slade, R. C. T.; Varcoe, J. R. *J. Mater. Chem.* **2003**, *13*, 712.
- Wang, Y.; Li, L.; Hu, L.; Zhuang, L.; Lu, J. T.; Xu, B. Q. *Electrochem. Commun.* **2003**, *5*, 662.
- Ogumi, Z.; Matsuoka, K.; Chiba, S.; Matsuoka, M.; Iriyama, Y.; Abe, T.; Inaba, M. *Electrochemistry* **2002**, *70*, 980.
- Agel, E.; Bouet, J.; Fauvarque, J. F. *J. Power Sources* **2001**, *101*, 267.
- Valade, D.; Boschet, F.; Ameduri, B. *J. Polym. Sci. Part A: Polym. Chem.* **2010**, *48*, 5801.
- Varcoe, J. R.; Slade, R. C. T.; Lam How Yee, E. *Chem. Commun.* **2006**, *13*, 1428.
- Robertson, N. J.; Kostalik, H. A.; Clark, T. J.; Mutolo, P. F.; Abruna, H. D.; Coates, G. W. *J. Am. Chem. Soc.* **2010**, *132*, 3400.
- Valade, D.; Boschet, F.; Roualdes, S.; Ameduri, B. *J. Polym. Sci. Part A: Polym. Chem.* **2009**, *47*, 2043.

17. Yan, J.; Hickner, M. A. *Macromolecules* **2010**, *43*, 2349.
18. Luo, Y.; Guo, J.; Wang, C.; Chu, D. *J. Power Sources* **2010**, *195*, 3765.
19. Huang, A.; Xia, C.; Xiao, C.; Zhuang, L. *J. Appl. Polym. Sci.* **2006**, *100*, 2248.
20. Vinodh, R.; Ilakkiya, A.; Elemathi, S.; Sangeetha, D. *Mater. Sci. Eng. B* **2010**, *167*, 43.
21. Zeng, Q. H.; Liu, Q. L.; Broadwell, I.; Zhu, A. M.; Xiong, Y.; Tu, X. P. *J. Membr. Sci.* **2010**, *349*, 237.
22. Gu, S.; Cai, R.; Luo, T.; Chen, Z. W.; Sun, M. W.; Liu, Y.; He, G. H.; Yan, Y. S. *Angew. Chem. Int. Ed.* **2009**, *48*, 6499.
23. Oyaizu, K.; Nakano, H.; Natori, J.; Tsuchida, E. *J. Electroanal. Chem.* **2011**, *498*, 232.
24. Wang, J.; Li, S.; Zhang, S. *Macromolecules* **2010**, *43*, 3890.
25. Guo, M.; Fang, J.; Xu, H.; Li, W.; Lu, X.; Lan, C.; Li, K. *J. Membr. Sci.* **2010**, *362*, 97.
26. Lin, B.; Qiu, L.; Lu, J.; Yan, F. *Chem. Mater.* **2010**, *22*, 6718.
27. Thomas, O. D.; Soo, K. J. W. Y.; Peckham, T. J.; Kulkarni, M. P.; Holdcroft, S. *Polym. Chem.* **2011**, *2*, 1641.
28. Wang, E. D.; Zhao, T. S.; Yang, W. W. *Int. J. Hydrogen Energy* **2010**, *35*, 2183.
29. Wu, Y.; Wu, C.; Varcoe, J. R.; Poynton, S. D.; Xu, T.; Fu, Y. *J. Power Sources* **2010**, *195*, 3069.
30. Vinodh, R.; Aravind Bhat, K.; Sangeetha, D. *J. Polym. Res.* **2011**, *18*, 1469.
31. Vinodh, R.; Purushothaman, M.; Sangeetha, D. *Int. J. Hydrogen Energy* **2011**, *36*, 7291.
32. Ding, F. C.; Wang, S. J.; Xiao, M.; Meng, Y. Z. *J. Power Sources* **2007**, *164*, 488.
33. Lin, Y. F.; Yen, C. Y.; Ma, C. C. M.; Liao, S. M.; Hung, C. H.; Hsiao, Y. H. *J. Power Sources* **2007**, *165*, 692.
34. Gnanakumar, G.; Lee, D. N.; Kim, P.; Nahm, K. S.; Elizabeth, R. N. *Eur. Polym. J.* **2008**, *44*, 2225.
35. Marx, S.; Gryp, P.; Neomagus, H.; Everson, R.; Keizer, K. *J. Membr. Sci.* **2002**, *209*, 353.
36. Kim, J. Y.; Mulmi, S.; Lee, C. H.; Park, H. B.; Chung, Y. S.; Lee, Y. M. *J. Membr. Sci.* **2006**, *283*, 172.
37. Cho, H. D.; Won, J.; Ha, H. Y.; Kang, Y. S. *Macromol. Res.* **2006**, *14*, 214.
38. Kreuer, K. D.; Paddison, S. J.; Spohr, E.; Schuster, M. *Chem. Rev.* **2004**, *104*, 4637.
39. Fu, R. Q.; Woo, J. J.; Seo, S. J.; Lee, J. S. *J. Power Sources* **2008**, *179*, 458.
40. Kato, M.; Sakamoto, W.; Yogo, T. *J. Membr. Sci.* **2008**, *311*, 182.
41. Kim, Y. M.; Choi, S. H.; Lee, H. C.; Hong, M. Z.; Kim, K.; Lee, H. I. *Electrochim. Acta.* **2004**, *49*, 4787.
42. Watanabe, M.; Uchida, H.; Emori, M. *J. Phys. Chem. B* **1998**, *102*, 3129.
43. Sacca, A.; Gatto, I.; Carbone, A.; Pedicini, R.; Passalacqua, E. *J. Power Sources* **2006**, *163*, 47.